

Date of publication xxxx 00, 0000, date of current version xxxx 00, 0000.

Digital Object Identifier 10.1109/ACCESS.2019.DOI

# Low Loss Ferrite Y-Junction Circulator based on Empty Substrate Integrated Coaxial Line at Ku-Band

LETICIA MARTINEZ<sup>1</sup>, VINCENT LAUR<sup>2</sup>, (Member, IEEE), ALEJANDRO L. BORJA<sup>3</sup>, (Member, IEEE), PATRICK QUÉFFÉLEC<sup>2</sup>, (Senior Member, IEEE), AND ANGEL BELENGUER<sup>1</sup>, (Senior Member, IEEE),

<sup>1</sup>Departamento de Ingeniería Eléctrica, Electrónica, Automática y Comunicaciones, Universidad de Castilla-La Mancha, Escuela Politécnica de Cuenca, Campus Universitario, 16071 Cuenca, Spain (e-mail: leticia.martinez@uclm.es, and angel.belenguer@uclm.es)

<sup>2</sup>Lab-STICC, University of Brest, 29238 Brest, France (e-mail: vincent.laur@univ-brest.fr)

<sup>3</sup>Departamento de Ingeniería Eléctrica, Electrónica, Automática y Comunicaciones, Universidad de Castilla-La Mancha, Escuela Politécnica de Albacete, Av. de España, s/n, 02071 Albacete, Spain (e-mail: alejandro.lucas@uclm.es)

Corresponding author: Angel Belenguer (e-mail: angel.belenguer@uclm.es).

This work was supported by the Ministerio de Economía y Competitividad, Spanish Government, under Research Project TEC2016-75934-C4-3-R, and by the Ministerio de Educación y Formación Profesional under the Fellowship Program for Training University Professors.

**ABSTRACT** A Y-junction circulator based on empty substrate integrated coaxial line (ESICL) technology is proposed in this paper. As ESICL is a novel transmission line, many of the common waveguide devices have not yet been developed in this technology, i. e. only filters, a power divider, a 90° hybrid directional coupler or transition structures have been presented but no non-reciprocal devices. In this paper, a ferrite based circulator has been designed and fabricated to operate at a central frequency of 12 GHz. Measurements performed with the help of an electromagnet confirms the stability of the circulator response under different DC biasing fields. Also, measurements with magnets have been done to integrate the circulator in communication systems. In addition, different temperature tests from 20° C to 90 °C have been carried out with the aim of checking the scattering parameters variations. The experimental results confirm the results obtained by the full wave simulations: insertion loss better than -1 dB isolation and return loss below -10 dB from 10 GHz to 14 GHz.

**INDEX TERMS** Empty substrate integrated coaxial line (ESICL), non-reciprocal device, ferrite, Y-junction circulator.

## I. INTRODUCTION

MICROWAVE circulators are passive electronic non-reciprocal devices with three or more ports where the energy is supplied to a port and routed to the next one in a defined direction, using the specific properties of magnetized ferrites (the ferrite is placed at the center of Y-junction). The other ports are isolated. Because of these unique properties, circulators are widely used in communication systems for the development of multiplexers, amplifiers or satellite receivers. The study of ferrites contained in waveguides was an important issue in the 1950s [1], [2]. Since the 1960s, the junction circulator with Y structure in waveguides, the effects of ferrite in microwaves and the integration of these circulators in other technologies such as stripline or microstrip technology have been studied [3]–[12].

Currently, there is a great interest in incorporating components manufactured in planar technologies into communications systems. This is because these devices are easy to manufacture and low cost since they are made from printed circuit boards (PCBs). The first waveguide integrated with this type of boards was the Substrate Integrated Waveguide (SIW) [13], where the wave propagates through the dielectric substrate of the PCB. This propagation makes the SIW an interesting structure at low frequencies due to its enhanced compactness but, due to the substrate, at high frequency its performance is reduced. As the first integrated waveguide, many circulators for different frequency bands have been designed [14]–[20].

In order to improve the performance of substrate integrated devices at high frequency, new planar structures were

proposed in which the propagation through the dielectric is avoided [21]–[23]. The latest reference is one of the most recent dielectricless integrated structures that have been proposed: Empty Substrate Integrated Coaxial Line (ESICL) [23]. Different coaxial lines as [24]–[26], have been studied, but these structures are not completely integrated, do not present transitions from/to other planar transmission lines and their manufacture is usually difficult and expensive. However, ESICL allows the integration of a rectangular coaxial line with PCB boards with low loss and negligible dispersion.

Being such a novel technology, few common waveguide devices have been developed based on it. To date, only two types of filters have been developed based on ESICL: a bandpass filter with shorted stubs [23], and a bandpass filter based on series resonators and impedance inverters [27]. Two transitions have also been presented: GCPW-to-ESICL transition [23] and compact microstrip to ESICL transition [28]. In addition, a power divider and a 90° hybrid directional coupler in ESICL technology have just been published [29]. Nevertheless, no non-reciprocal devices such as circulators have been proposed to date. Therefore, in this article the first Y-junction circulator based on ESICL technology is presented. By these means, it is possible to obtain more complex ESICL-only based devices. Without this novel, and completely embedded ESICL circulator, the use of non-reciprocal devices in combination with ESICL-based elements would require the intensive use of transitions to other planar lines.

## II. ESICL CIRCULATOR STRUCTURE AND DESIGN PROCESS

### A. ESICL CIRCULATOR STRUCTURE

An ESICL line is shown in Fig. 1. As it can be seen, it is composed of five PCB layers. The central layer (3 in Fig. 1) is the layer where the central conductor of the integrated coaxial line is located. Layers 2 and 4 are responsible for separating the outer conductor of the coaxial line from the inner conductor. Finally, layers 1 and 5 are the covers that prevent EM Propagation out of the structure.

The circulator designed is a junction circulator with a Y-structure (120° difference between its three branches) based on the multilayer configuration proposed in [23]. The intersection between the three branches is covered by two ferrites: one above and one below (see Fig. 2a). One should note that this structure can be approximated as an integrated stripline.

Due to the structure of the ESICL, the circulator is located in the inner conductor of the coaxial line. Therefore, the ferrites are placed between the central layer and layers 1 and 5, respectively, and their height, denoted as  $h_{ferrite}$ , is determined by the gap between them (see Fig. 2b).

In general, the initial radius of the ferrite and the width of the stripline connected to the ferrite resonator can be calculated by applying the following equations (1) and (2), as it was proposed in [5], where a Bosma model is applied to the stripline. In this procedure, Bosma consider only TM

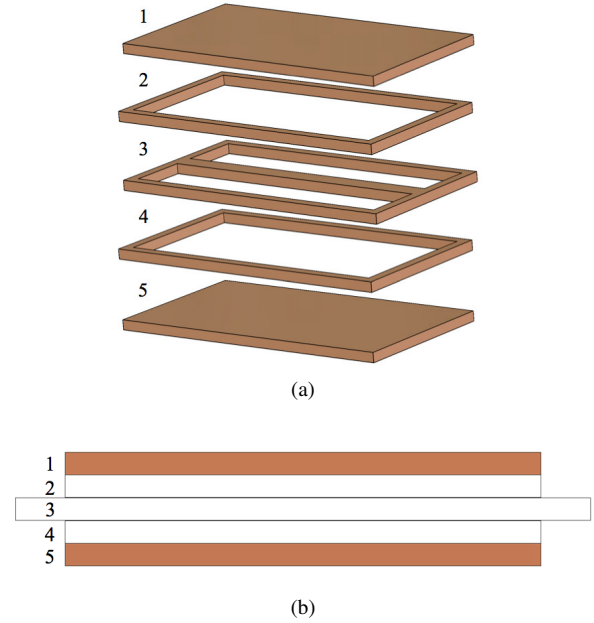


**FIGURE 1.** Structure of an ESICL (two covers with three inner layers). (a) 3D view of the layers of an ESICL. (b) Profile view of an ESICL.

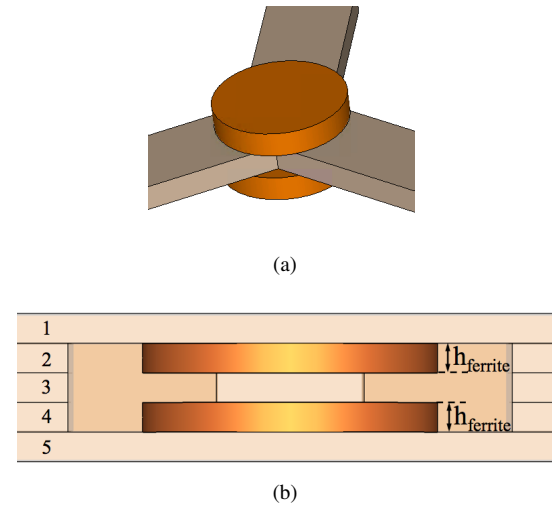


**FIGURE 2.** Structure of an ESICL Y-Junction Circulator. (a) Detail of the Y-Junction Circulator. (b) Cross-section Circulator ESICL.

resonance modes that are independent of thickness (if this thickness is sufficiently small).

$$\frac{R}{\lambda} = \frac{1.84}{2\pi\sqrt{\mu_{eff}\epsilon}} \quad (1)$$

$$\frac{\kappa}{\mu} = \sqrt{3} \frac{w_{circulator}}{\lambda} \quad (2)$$

where  $R$  is the radius of the ferrite disk,  $\lambda$  is the free space wavelength,  $\mu_{eff}$  is the effective specific gyrotropic permeability,  $\epsilon$  is the relative complex permittivity of the ferrite,  $\kappa$  and  $\mu$  are the parameters of the Polder tensor and  $w_{circulator}$  is the width of the line connected to the ferrite. More specifically,  $\mu$  and  $\kappa$  are calculated by using the Polder

model with the parameters of Table 1, considering that the internal magnetic field is zero. In this case,  $\mu=1$ ,  $\kappa=0.7323$  and therefore  $\mu_{eff}$  is calculated as  $\mu_{eff}=(\mu^2-\kappa^2)/\mu=0.4638$ . Other approaches to design stripline circulators can be also used to obtain the geometrical parameters of the ferrite. For example, the results of [30] could be applied, where the key equations are revisited to include the effect of higher order stripline modes.

## B. CIRCULATOR DESIGN PROCESS

This subsection presents information that can be used to redesign the circulator, e.g. for operation at a different central frequency. The design procedure can be summarized as follows:

First, the working frequency of the ESICL Y-junction circulator is selected. As it was shown in [28], this transmission line can work at high frequency with high efficiency and low losses i.e. insertion losses below 1 dB and return losses better than 18 dB between 10 GHz and 16 GHz. Therefore, a central frequency of 12 GHz for the circulator has been chosen. These types of circulators are operated far from gyromagnetic resonance (usually above), in a frequency region where magnetic losses are very low. A ferrite with moderate saturation magnetization,  $M_s$ , is needed in order to avoid low field magnetic losses that are, for a given operation frequency, proportional to  $M_s$ . Considering also the chosen frequency of operation, the selected ferrite is Y101 from Exxelia Temex, a ferrite composed of yttrium, iron and garnet that operates at the required frequencies. Its characteristics can be seen in Table 1 where  $M_s$  is the saturation magnetization,  $g_{eff}$  is the effective Landé factor,  $\Delta H$  is the ferromagnetic resonance line width,  $\Delta H_{eff}$  is the effective line width,  $\Delta H_k$  is the spin waveline width and  $\epsilon$  is the relative complex permittivity of the ferrite.

TABLE 1. Y101 Proprieties

Type	$M_s$	$g_{eff}$	$\Delta H$	$\Delta H_{eff}$	$\Delta H_k$	$\epsilon$
Y101	1820 G	2.02	18 Oe	3 Oe	1.5 Oe	15

Once the ferrite properties are known, the ferrite and the transmission line dimensions can be determined. Since the calculation of the radius makes reference to a stripline junction circulator and the size of the inner conductor is limited to the specifications of ESICL structure, both the calculated radius of the ferrite disk and the calculated width and length of the inner conductor of the coaxial line in the circulator will be starting points for their true values. The values obtained will be optimized using a full-wave electromagnetic simulator to achieve a correct operation of the circulator in this novel technology.

A PCB of Rogers 4003C<sup>TM</sup> with  $\epsilon_r = 3.55$ , 0.813 mm thickness and 26.5  $\mu\text{m}$  (17.5  $\mu\text{m}$  copper + 9  $\mu\text{m}$  galvanic) of total metallization has been chosen to manufacture the ESICL circulator. The value of  $h_{ferrite}$  is the sum of the height of the substrate and the total metallization on each of

its faces. In this case, the height of the ferrite is  $h_{ferrite} = 0.866$  mm.

The initial radius of the ferrite resonator  $R$  and width of the inner conductor  $w_{circulator}$  were calculated by applying (1) and (2). These formulas gave initial values  $R = 2.09$  mm and  $w_{circulator} = 4.12$  mm. These dimensions act as starting values for full-wave electromagnetic simulations. The dimension  $l_1$ , see Fig. 3a, is optimized to match the impedance of the circulator to the impedance of the microstrip transition and therefore minimize the feeding effects on the circulator response in the final design (the width of the feeding line,  $w_{ci}$ , is 1.82 mm).

To get the final geometric characteristics of the circulator, the whole structure (without transitions) has been optimized. A Trust Region Framework Algorithm with the following goals has been applied:  $S_{11} < -20$  dB,  $S_{21} > -0.5$  dB and  $S_{31} < -20$  dB to achieve the desired behavior with CST Studio Suite between 10 GHz and 14 GHz.

The initial and final dimensions of the circulator are shown in the Table 2. The design after the optimization of the radius of the ferrites and the size of the inner conductor of the circulator is shown in Fig. 3a. In order to connect the circulator to a Vector Network Analyzer (VNA), three compact microstrip line to ESICL transitions have been added to the Y-junction circulator following [28] (see Fig. 3b). The response of the exact transition we have used in this work can be seen in Fig. 5 of [28].

TABLE 2. Y-Junction Circulator Dimensions

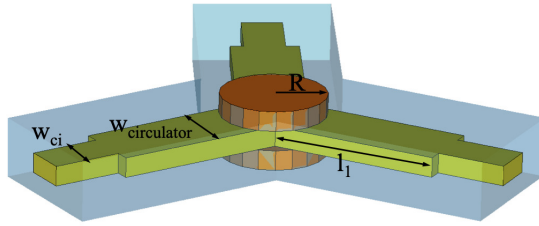
	$R$	$w_{circulator}$	$l_1$
Initial values (mm)	2.09	4.12	8
Final values (mm)	2.42	4.05	7.26

The Y-junction circulator based on ESICL line is shown in Fig. 3b and its simulated results, without transitions, can be observed in Fig. 4. The return loss ( $S_{11}$ ) and isolation ( $S_{21}$ ) are below -10 dB from 8.79 GHz to 13.49 GHz (39.16% fractional bandwidth), below -15 dB from 9.78 GHz to 13.11 GHz (27.75% fractional bandwidth) and insertion loss,  $S_{31}$ , is around 0.2 dB in this frequency ranges.

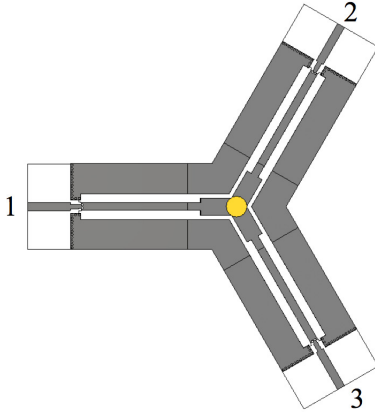
Finally, the electric field distribution inside the circulator at 12 GHz has been represented in Fig. 5. In this figure, it can be seen how the electromagnetic fields circulate around the polarized ferrite.

## III. EXPERIMENTAL RESULTS

The Y-Junction Circulator based on ESICL has been manufactured in order to experimentally validate the design presented in Section II-B. To manufacture the prototype, as it has already been said, a PCB of Rogers 4003C<sup>TM</sup> with  $\epsilon_r = 3.55$ , 0.813 mm thickness and 26.5  $\mu\text{m}$  of total metallization has been chosen. A LPKF Protolaser U3 machine, following standard PCB processes, has been used to mechanize the PCB (cutting, drilling and copper removal). Figures 6a and 6b show the central layer of the prototype with the ferrites stuck to the junction of the branches of the circulator with



(a)



(b)

**FIGURE 3.** ESICL Y-Junction Circulator design. (a) 3D view of the Y-Junction Circulator. (b) Top view of the ESICL Y-Junction Circulator design with microstrip-to-ESICL transitions (central layer).

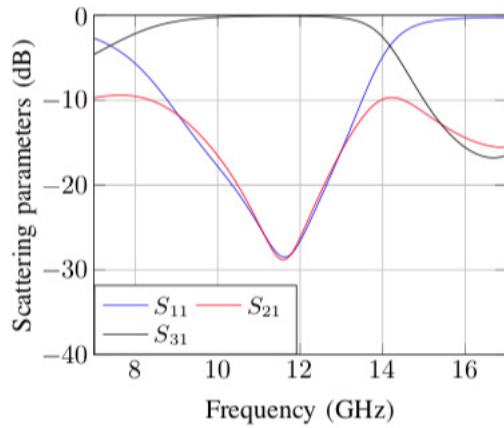


**FIGURE 4.** Simulation results for the ESICL Y-Junction Circulator without transitions.

cianoacrylate glue. Fig. 6c shows the complete junction circulator based on ESICL transmission line. It can be seen that the different layers are joined with screws and nuts. To perform the measurements, one of the ports of the circulator is loaded with 50  $\Omega$ -load (from a Keysight calibration kit: 85052D).

To characterize this circulator, three different procedures have been made: measurements with an electromagnet, measurements with magnets and a temperature test with magnets.

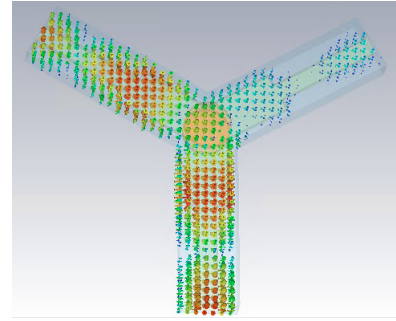
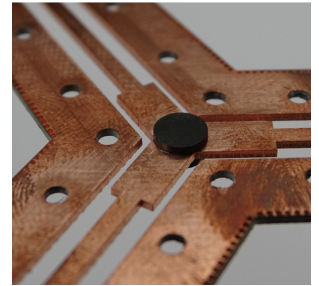


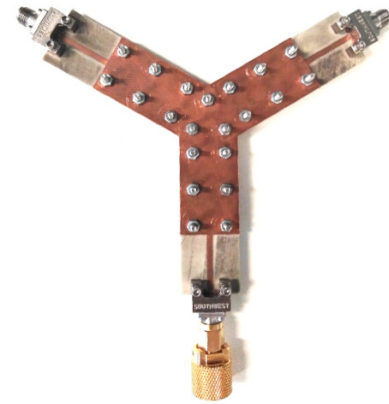
**FIGURE 5.** Electric field distribution at 12 GHz when excited at port 1.



(a)



(b)



(c)

**FIGURE 6.** Manufactured ESICL Y-Junction Circulator Prototype. (a) Top view of the central layer. (b) Ferrites above and below of the junction circulator. (c) Top view of the ESICL Y-Junction Circulator.

#### A. MEASUREMENTS WITH AN ELECTROMAGNET

First, measurements with an electromagnet have been made to find out how much DC biasing field is necessary for the correct operation of the circulator. In addition, it is important to know if the response of the circulator is stable once the minimum strength of the magnetic biasing field has been reached.

Measurements have been performed with an TE2M electromagnet, an Agilent Technologies E8364A PNA Series Network Analyzer, which has been calibrated using our custom Thru-Reflect-Line (TRL) calibration kit, following [31] and [32] (see Fig. 7). Thus, the measurement planes are



moved inside the ESICL, so that the response of the actual ESICL device is actually recovered.

Although this calibration is possible, it is necessary to remark that the microstrip-to-ESICL transition is a complex structure, and it is highly probable that the manufactured transitions of each standard and the circulator show slightly different performances. In other words, the calibration is not perfect. It can provide a good estimation of the insertion loss, but results for return loss, which is very sensitive to errors, are less precise. As a result, measured return loss will be always under what is predicted by simulations.

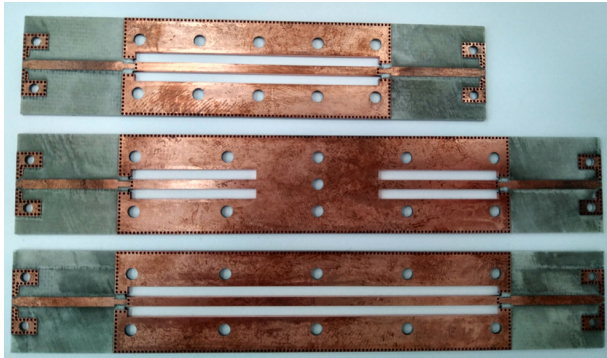


FIGURE 7. Central layer of the custom TRL calibration kit.

In Fig. 8 the measurement procedure is observed. The circulator is inserted between the poles of the electromagnet, held by a clamp, and a probe (Hall effect Gaussmeter) placed in the center of the circulator indicates the surrounding magnetic biasing field.

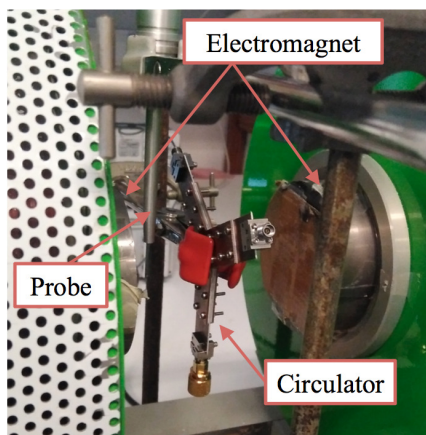


FIGURE 8. ESICL Y-Junction Circulator set in the air gap of the electromagnet.

The magnetic biasing field applied to perform the measurements was varied from 1000 Oe to 2600 Oe in steps of 200 Oe. Fig. 9 shows the results obtained for the circulator with a port loaded with  $50 \Omega$  -load. It can be seen how from 1200 Oe to 2600 Oe, between 10 GHz and 14 GHz,  $S_{12}$  is above -1 dB while  $S_{11}$ ,  $S_{21}$  and  $S_{22}$  are below -10 dB. The response of the circulator applying a magnetic biasing field of 1400 Oe

obtained is very similar to that obtained with higher fields, being a stable response from this value.

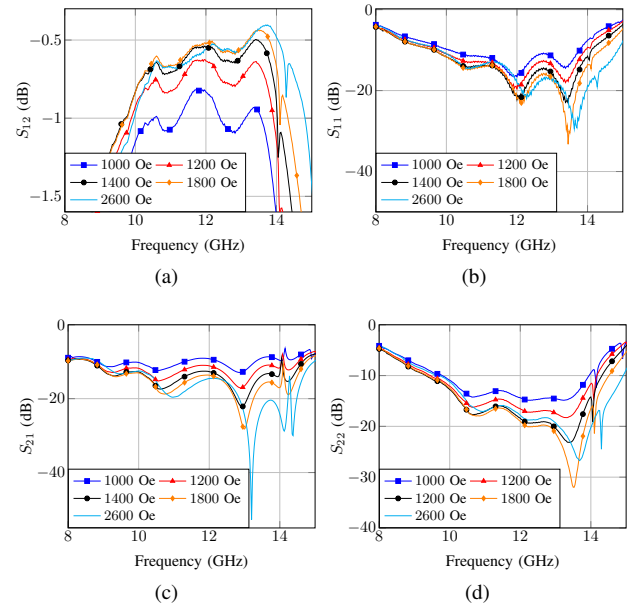


FIGURE 9. Measurement comparisons for different electromagnetic fields

Fig. 10 compares the simulated results with losses with those obtained in the experiment with the electromagnet generating a magnetic biasing field of 1600 Oe. There are differences between the amplitudes of  $S_{21}$  and  $S_{11}$  obtained in simulation and those measured, especially from 10 GHz, due to the effect of the transition, that has not been completely corrected with the TRL calibration. Although in this case a frequency shift is not observed, the existing uncertainty about the value of the permittivity, which according to the manufacturer can vary by 5% of its nominal value, can cause a frequency shift of up to 250 MHz in this frequency band, as we have verified in different simulations. Despite the differences observed, the performance of the circulator measured is very similar to that of the simulated circulator.

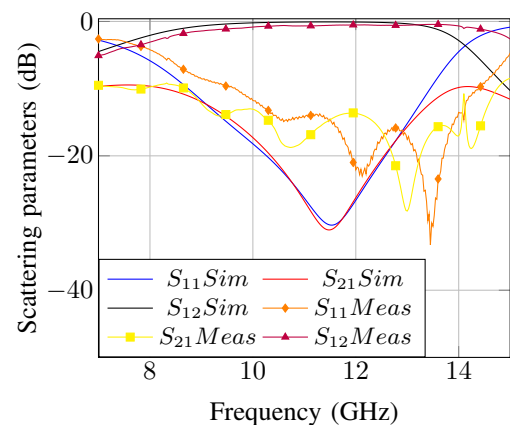
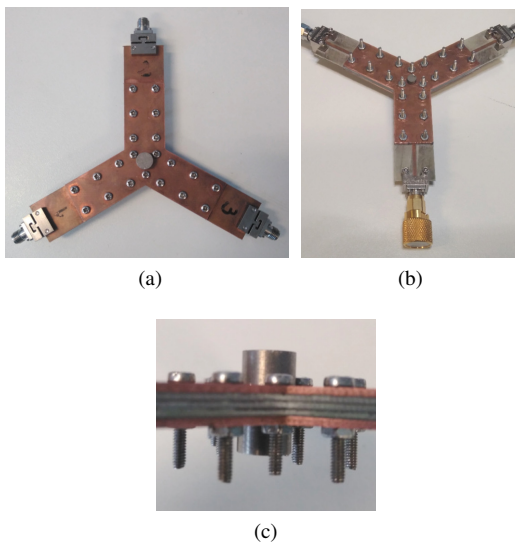


FIGURE 10. Simulated S-parameters modulus with losses and measured ones for the ESICL junction Circulator biased by an electromagnet (1600 Oe).

Table 3 shows the results obtained for the presented circulator compared with other circulators manufactured in an equivalent technology (SIW) and one circulator manufactured in rectangular waveguide (RWG). As it can be seen, the proposed ESICL Y-junction circulator presents the best performance in terms of measured insertion loss, only below the conventional rectangular waveguide as expected. However, for planar technologies the use of 3D structures is restricted due its difficult integration. In addition, the fractional bandwidth, return loss and isolation losses are similar for all structures compared. Therefore, this circulator complies with the standards that could be required in a real application.

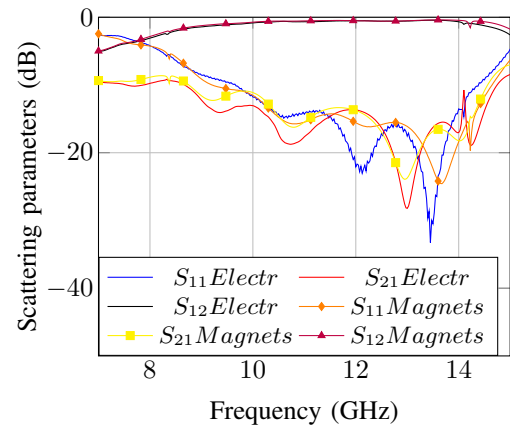
### B. MEASUREMENTS WITH PERMANENT MAGNETS

Once the proper behavior of the circulator is known, measurements have been made with two SmCo cylindrical magnets of 8 mm diameter and 4.2 mm height which generate a magnetic field of 1600 Oe. The magnetic field has been measured at the distance corresponding to the height of the device with a Gaussmeter GN20000E from TE2M. In this case, the circulator response has been made with a Rohde & Schwarz ZVA67 Vector Network Analyzer that has also been calibrated using the same custom TRL calibration kit. In Fig. 11 the circulator, with the magnets centered in the junction, is shown.



**FIGURE 11.** ESICL Junction Circulator Prototype with magnets. (a) Bottom view. (b) Top view. (c) Cross-section. Detail magnets 8 mm diameter and 4.2 mm height

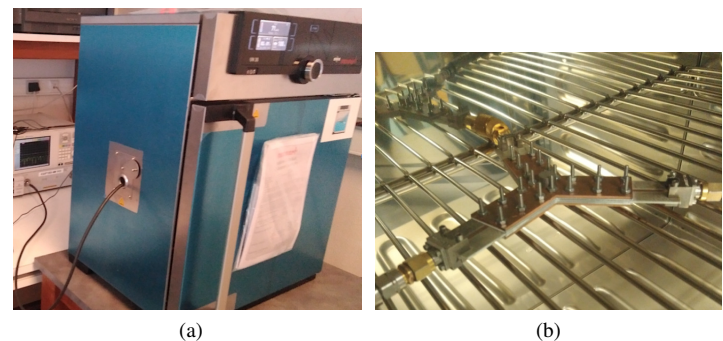
The comparison between the results obtained with the electromagnet, generating a magnetic biasing field of 1600 Oe, and measurements with magnets of 8 mm diameter and 4.2 mm height are shown in Fig. 12. The results show a good agreement. The insertion loss obtained is above 1 dB between 10 GHz and 14 GHz, while the return loss is below -10 dB in all cases i. e.  $S_{11}$  and  $S_{21}$ .



**FIGURE 12.** Measurements for the ESICL junction Circulator with the electromagnet generating a magnetic biasing field of 1600 Oe and measurements for the ESICL junction Circulator with magnets of 8 mm diameter and 4.2 mm height.

### C. TEMPERATURE TEST

After checking the correct operation of the Y-junction circulator with magnets, a new set of measurements has been performed to evaluate the stability of the circulator under different temperature scenarios. The assembly of the measurement is shown in the Fig. 13. The circulator with two magnets of 8 mm  $\phi$  and 4.2 mm height were introduced inside a Memmert UN30 oven and measured with an Agilent Technologies E8364A PNA Series Network Analyzer, which has also been calibrated using our custom TRL calibration kit.

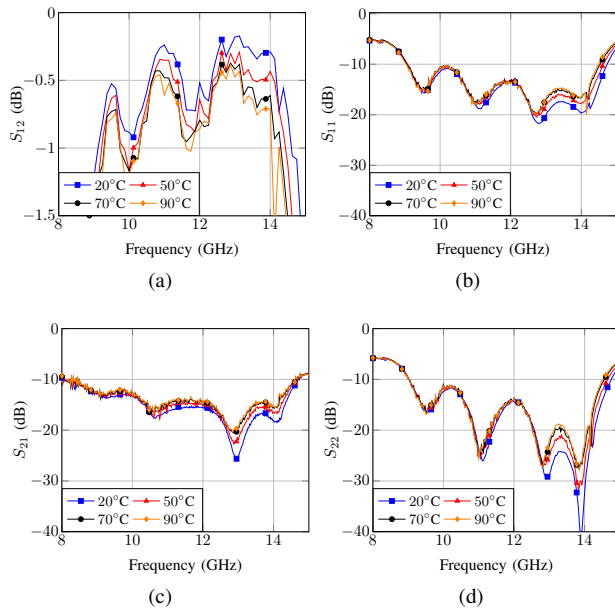


**FIGURE 13.** Temperature Test. (a) Union of the oven and the analyzer (b) Circulator inside the oven.

The temperature test was performed from 20°C (room temperature) to 90°C in steps of 10°C. The results obtained can be observed in Fig. 14. The difference between  $S_{12}$  at 20°C and  $S_{12}$  at 90°C is 0.35 dB. Isolation and return loss prove to be very stable in this temperature range. The response of the Y-junction circulator based on ESICL at 90°C still has insertion losses lower than 1 dB, thus it can be concluded that the ESICL circulator exhibits a very stable response with temperature. This reasonable stability is mainly provided by the low temperature coefficient of the magnets used, from the provider Magpy, which is typically  $\Delta B_r / (B_r \times \Delta T) = -0.035\% / ^\circ\text{C}$ .

TABLE 3. Circulators comparison

	Technology	$f_c$ (GHz)	% BW	IL (dB)	RL (dB)	ISO (dB)
[14]	SIW	35	10.2 sim	0.6 sim	20 sim	20 sim
[15]	SIW	21	18	1.3	15	15
[16]	SIW	36	N.A.	0.3 sim	25 sim	25 sim
[17]	SIW	10.45	N.A.	1 sim	15 sim	15 sim
[18]	SIW	32	5 sim	N. A.	N. A.	N. A.
ESICL circulator	ESICL	12	33.3	1	10	10
[33]	RWG	41	9.7	0.87	20	20
[30]	STRIPLINE	10.815	41.6 sim	N.A.	15	15

FIGURE 14. Comparison of measurements for different temperatures with two magnets of 8 mm  $\phi$  and 4.2 mm height.

#### IV. CONCLUSION

In this paper, Y-junction circulator based on ESICL has been designed, fabricated and measured. Different types of measurements have been made to check its behavior in different situations. The measurements made with the electromagnet show the correct operation of the circulator for different magnetic fields with insertion losses lower than 1 dB and isolation greater than 10 dB between 10 GHz and 14 GHz. Measurements have also been made with magnets with different magnetization strengths. The responses obtained in this case show good agreement with the responses obtained with the electromagnet. Finally, a temperature test has been performed. The results obtained show that the response of the junction circulator is barely affected if temperature ranges from 20°C to 90°C.

#### REFERENCES

- [1] N. G. Sakiotis and H. N. Chait, "Ferrites at microwaves," Proceedings of the IRE, vol. 41, no. 1, pp. 87–93, Jan. 1953.
- [2] N. G. Sakiotis and H. N. Chait, "Properties of ferrites in waveguides," Trans. of the IRE Prof. Group on Microw. Theory Techn., vol. 1, no. 2, pp. 11–16, Nov. 1953.
- [3] F. M. Aitken and R. McLean, "Some properties of the waveguide Y-circulator," Electrical Engineers, Proceedings of the Institution of, vol. 110, no. 2, pp. 256–260, Feb. 1963.
- [4] J. B. Davies, "An Analysis of the m-port symmetrical H-plane waveguide junction with central ferrite post," IRE Trans. Microw. Theory Techn., vol. 10, no. 6, pp. 596–604, Nov. 1962.
- [5] H. Bosma, "On stripline Y-circulation at UHF," IEEE Trans. Microw. Theory Techn., vol. 12, no. 1, pp. 61–72, Jan. 1964.
- [6] C. E. Fay and R. L. Comstock, "Operation of the ferrite junction circulator," IEEE Trans. Microw. Theory Techn., vol. 13, no. 1, pp. 15–27, Jan. 1965.
- [7] Y. Akaiwa, "Operation modes of a waveguide Y circulator (short papers)," IEEE Trans. Microw. Theory Techn., vol. 22, no. 11, pp. 954–960, Nov. 1974.
- [8] J. Helszajn and F. C. Tan, "Design data for radial-waveguide circulators using partial-height ferrite resonators," IEEE Trans. Microw. Theory Techn., vol. 23, no. 3, pp. 288–298, Mar. 1975.
- [9] C. Schieblich and J. H. Hinken, "Ka-band Y-circulators in integrated waveguide technology," Electron. Lett., vol. 19, no. 17, pp. 665–666, Aug. 1983.
- [10] V. Laur, G. Verissimo, P. Quéffelec, L. A. Farhat, H. Alaeddine, E. Laroche, G. Martin, R. Lebourgeois, and J. P. Ganne, "Self-biased Y-junction circulators using lanthanum- and cobalt-substituted strontium hexaferrites," IEEE Trans. Microw. Theory Techn., vol. 63, no. 12, pp. 4376–4381, Dec. 2015.
- [11] V. Laur, R. Lebourgeois, E. Laroche, J. Mattei, P. Queffelec, J. Ganne, and G. Martin, "Study of a low-loss self-biased circulator at 40 GHz: influence of the temperature," in IEEE Int. Microw. Symp., San Francisco, May. 2016.
- [12] L. Qassim, V. Laur, P. Queffelec, and R. Lebourgeois, "Ferrimagnetic garnets for low temperature co-fired ceramics microwave circulators," in IEEE Int. Microw. Symp., Philadelphia-USA, Jun. 2018.
- [13] D. Deslandes and K. Wu, "Integrated microstrip and rectangular waveguide in planar form," IEEE Microw. Compon. Lett., vol. 11, no. 2, pp. 68–70, Feb. 2001.
- [14] Z. Shi and Z. Shao, "Design of Ka-band substrate integrated waveguide circulator," in Int. Conf. on Comput. Problem-Solving, Dec. 2010, pp. 260–262.
- [15] W. D'Orazio, K. Wu, and J. Helszajn, "A substrate integrated waveguide degree-2 circulator," IEEE Microw. Compon. Lett., vol. 14, no. 5, pp. 207–209, May 2004.
- [16] C. Huang, X. Wang, and L. Deng, "Design of Ka-band high-performance circulator," in 2014 IEEE Int. Conf. on Electron Devices and Solid-State Circuits, Jun. 2014, pp. 1–2.
- [17] M. Almalkawi, L. Zhu, and V. Devabhaktuni, "Magnetically tunable substrate integrated waveguide bandpass filters employing ferrites," in 2011 Int. Conf. on Infrared, Millimeter, and Terahertz Waves, Oct. 2011, pp. 1–2.
- [18] J. He, K. Gao, and Z. Shao, "A novel compact Ka-band high-rejection diplexer based on substrate integrated waveguide," in 2012 Int. Conf. on Comput. Problem-Solving (ICCP), Oct. 2012, pp. 193–197.
- [19] X. Jiang, C. J. You, and Z. Shao, "A compact X-band circulator with embedded feed line based on substrate integrated waveguide," in 2013 Int. Conf. on Comput. Problem-Solving (ICCP), Oct. 2013, pp. 58–60.



- [20] V. Laur, J. Mattei, G. Vérissimo, P. Queffelec, R. Lebourgeois, and J. Ganne, "Application of molded interconnect device technology to the realization of a self-biased circulator," *Journal of Magnetism and Magnetic Materials*, vol. 404, pp. 126–132, Apr. 2016.
- [21] F. Parment, A. Ghiotto, T. P. Vuong, J. M. Duchamp, and K. Wu, "Air-filled substrate integrated waveguide for low-loss and high power-handling millimeter-wave substrate integrated circuits," *IEEE Trans. Microw. Theory Techn.*, vol. 63, no. 4, pp. 1228–1238, Apr. 2015.
- [22] A. Belenguer, H. Esteban, and V. E. Boria, "Novel empty substrate integrated waveguide for high-performance microwave integrated circuits," *IEEE Trans. Microw. Theory Techn.*, vol. 62, no. 4, pp. 832–839, Apr. 2014.
- [23] A. Belenguer, A. L. Borja, H. Esteban, and V. E. Boria, "High-performance coplanar waveguide to empty substrate integrated coaxial line transition," *IEEE Trans. Microw. Theory Techn.*, vol. 63, no. 12, pp. 4027–4034, Dec. 2015.
- [24] I. Llamas-Garro, M. J. Lancaster, and P. S. Hall, "Air-filled square coaxial transmission line and its use in microwave filters," *IEEE Proceedings - Microw. Antennas and Propag.*, vol. 152, no. 3, pp. 155–159, Jun. 2005.
- [25] M. J. Lancaster, J. Zhou, M. Ke, Y. Wang, and K. Jiang, "Design and high performance of a micromachined K-band rectangular coaxial cable," *IEEE Trans. Microw. Theory Techn.*, vol. 55, no. 7, pp. 1548–1553, Jul. 2007.
- [26] N. Jastram and D. S. Filipovic, "PCB-Based prototyping of 3-D micromachined RF subsystems," *IEEE Trans. Antennas Propag.*, vol. 62, no. 1, pp. 420–429, Jan. 2014.
- [27] A. L. Borja, A. Belenguer, H. Esteban, and V. E. Boria, "Design and performance of a high- $Q$  narrow bandwidth bandpass filter in empty substrate integrated coaxial line at Ku-band," *IEEE Microw. Compon. Lett.*, vol. 27, no. 11, pp. 977–979, Nov. 2017.
- [28] F. Quiles, A. Belenguer, J. A. Martinez, V. Nova, H. Esteban, and V. E. Boria, "Compact microstrip to empty substrate integrated coaxial line transition," *IEEE Microw. Wirel. Compon. Lett.*, vol. 28, no. 12, pp. 1080–1082, 2018.
- [29] J. M. Merello, V. Nova, C. Bachiller, J. R. Sánchez, A. Belenguer, and V. E. B. Esbert, "Miniaturization of power divider and 90° hybrid directional coupler for C-Band applications using empty substrate-integrated coaxial lines," *IEEE Trans. Microw. Theory Techn.*, vol. 66, no. 6, pp. 3055–3062, Jun. 2018.
- [30] S. I. Shams, M. Elsaadany, and A. A. Kishk, "Including stripline modes in the y-junction circulators: Revisiting fundamentals and key design equations," *IEEE Transactions on Microwave Theory and Techniques*, vol. 67, no. 1, pp. 94–107, Jan 2019.
- [31] M. D. F. Berlanga, J. A. B. Garrido, L. M. Cano, H. E. González, and Á. B. Martínez, "Thru-reflect-line calibration for empty substrate integrated waveguide with microstrip transitions," *Electronics Letters*, vol. 51, no. 16, pp. 1274–1276, 2015.
- [32] M. Fernandez, J. A. Ballesteros, J. A. Martinez, J. J. de Dios, and A. Belenguer, "Wide-bandwidth thru-reflect-line calibration for empty substrate integrated coaxial line with GCPW transitions," *Microw Opt Technol Lett.*, no. 61, pp. 292–296, 2019.
- [33] V. Laur, G. Vérissimo, P. Quéffelec, L. A. Farhat, H. Alaeddine, E. Laroche, G. Martin, R. Lebourgeois, and J. P. Ganne, "Self-biased y-junction circulators using lanthanum- and cobalt-substituted strontium hexaferrites," *IEEE Transactions on Microwave Theory and Techniques*, vol. 63, no. 12, pp. 4376–4381, Dec. 2015.



LETICIA MARTINEZ received the Technical Telecommunication Engineering degree from the Universidad de Castilla-La Mancha (UCLM), Spain in 2009, and the Telecommunication Master from the Universidad Politécnica de Madrid (UPM), Spain, in 2012. She received the Ph. D. degree in physics and mathematics from the Universidad de Castilla-La Mancha (UCLM), Spain, under the Fellowship Program for Training University Professors (FPU) in 2019. She is currently a Post-Doctoral Fellow at the Lab-STICC Laboratory in Brest, France. Her research interests include waveguides, substrate integrate waveguide, EM metamaterials, reconfigurable devices and the application of 3D printable materials in microwave bands.



VINCENT LAUR (M'15) received the Ph.D. degree in electronics from the University of Brest, Brest, France, in 2007. In 2008, he was a Post-Doctoral Fellow at the XLIM Laboratory, Limoges, France. He is currently an Associate Professor at the Lab-STICC Laboratory, Brest, France. He has published more than 90 papers in peer-reviewed international journals and conference proceedings and frequently acts as a reviewer for several technical publications. His research interests are focused on the characterization, modeling, and integration of functional materials (ferroelectrics, ferromagnetics, ferrites, etc.) for microwave applications. He is also invested in the application of new technologies (3D printing, 3D metallization, Molded Interconnect Devices, nanomaterials ...) to the microwave domain.



ALEJANDRO L. BORJA (M'15) received the M.Sc. degree in telecommunication engineering and the Ph.D. degree from the Universidad Politécnica de Valencia, Valencia, Spain, in 2005 and 2009, respectively. From 2005 to 2006, he was with the University of Birmingham, Birmingham, U.K. From 2007 to 2008, he was with the Université de Lille 1, Lille, France. Since 2009, he has been with the Universidad de Castilla-La Mancha, Spain, where he is an Assistant Lecturer. He has published more than 60 papers in peer-reviewed international journals and conference proceedings, and frequently acts as a reviewer for several technical publications. In 2012, he served as a Lead Guest Editor for a special issue of the *International Journal of Antennas and Propagation*. His research interests include EM metamaterials, substrate integrate waveguide, and reconfigurable devices and their applications in microwave and millimetric bands. Dr. Borja was the recipient of the 2008 CST short paper award.



PATRICK QUÉFFÉLEC (M'99-SM'07) received his PhD degree in Electronics from the Université de Bretagne Occidentale, Brest, France, in 1994 and his Habilitation à diriger des recherches [accreditation to supervise research] in 2002. He is now a professor at the Laboratory of Sciences and Techniques of Information, Communication and Knowledge (Lab-STICC), a research unit associated with the Centre National de la Recherche Scientifique (UMR CNRS n°6285). His research activities concern electromagnetic wave propagation in heterogeneous and anisotropic media. He works on developing new approaches in materials and measurements for microwave ferrites and devices. Motivated by the applications of new magnetic materials in non-reciprocal or tuneable devices, in antennas, he is investigating the fundamental properties of magnetoelectric nanocomposites at microwave frequencies. He has authored and co-authored over 145 refereed journal and conference papers, 5 patents and 2 book chapters. He gave 11 invited talks and frequently acts as a reviewer for numerous international technical publications.





ANGEL BELENGUER (M'04–SM'14) received his degree in telecommunications engineering from the Universidad Politecnica de Valencia (UPV), Spain, in 2000, and his Ph.D. degree, also from the UPV, in 2009. He joined the Universidad de Castilla-La Mancha in 2000, where he is now Profesor Titular de Universidad in the Departamento de Ingenieria Electrica, Electronica, Automatica y Comunicaciones. He has authored or co-authored more than 50 papers in peer-reviewed international journals and conference proceedings and frequently acts as a reviewer for several international technical publications. His research interests include methods in the frequency domain for the full-wave analysis of open-space and guided multiple scattering problems, EM metamaterials, and Empty Substrate Integrated Waveguide (ESIW) devices and their applications.

• • •